Nanoscale

COMMUNICATION

View Article Online
View Journal | View Issue

Open Access Article. Published on 21 October 2016. Downloaded on 9/13/2025 2:09:01 PM.
This article is licensed under a Creative Commons Attribution 3.0 Unported Licence.

Cite this: *Nanoscale*, 2016, **8**, 18630

Received 16th September 2016,
Accepted 20th October 2016

DOI: 10.1039/c6nr07336k

www.rsc.org/nanoscale

Three-minute synthesis of sp^3 nanocrystalline carbon dots as non-toxic fluorescent platforms for intracellular delivery†

Stephen A. Hill,[a] David. Benito-Alifonso,[a] David J. Morgan,[b] Sean A. Davis,[a] Monica Berry[a] and M. Carmen Galan*[a]

A one-pot, three-minute, gram-scale synthesis of novel sp^3-nanocrystalline, water-soluble, and fluorescent carbon dots (FCDs), from simple and cheap sugar starting materials is described. Mechanism studies showed that NH_2-FCD formation proceeds *via* a crucial imine intermediate derived from reaction between a sugar hemiacetal and an amine. Moreover, we successfully demonstrate the utility of lactose functionalized FCDots (Lac-FCDots) as non-toxic fluorescent intracellular delivery vehicles.

The application of nanotechnology to biological and medical problems has seen an explosion of research in recent years.[1] Functional nanomaterials that incorporate biomolecules as recognition motifs have become very useful for cargo delivery, sensing and catalysis.[2] Nanomaterials with novel optical, electronic and surface properties that exhibit a low cytotoxicity profile are particularly valuable platforms for tracking biomolecules within the complex cellular environment, and in the development of novel therapies and *in vivo* diagnostics.[3]

Carbohydrate–protein recognition processes are mediated by multivalent interactions that help achieve higher affinity as well as higher specificity.[4] Glycan-coated nanodots have been validated as multivalent tools to screen for protein–carbohydrate interactions associated with inter- and intracellular recognition processes.[5] Our group recently demonstrated that the type of glycan presented on a fluorescent CdSe/ZnS quantum dot (QD) can enable control of nanodot uptake and intracellular localization in cervical cancer HeLa cells, and in immortalised corneal epithelial cells.[6] Although we showed that glycan density mitigates the inherent toxicity of CdSe QDs, these QDs remain less than ideal for *in vivo* applications. In order to broaden the scope of functional nanomaterials for biomedical purposes, it is of the utmost importance to develop non-toxic and stable nanomaterials that can be used over long periods of exposure.

Carbon dots (CDs) are a relatively new material that have attracted significant interest since their serendipitous discovery in 2004 due to their unique and tuneable optical properties, which are comparable and sometimes superior to those of semiconductor QDs.[7] Their photoluminescence (PL) properties, chemical inertness, excellent water solubility, low cost of fabrication, and general minimal toxicity suggest wide-ranging potential uses, including *in vivo* applications.[8] Current CD fabrication methods can be either top-down (from bulk carbon sources) or bottom-up (seeding from molecular precursors) and generally result in CDs containing an amorphous or graphitic sp^2 crystalline core with a range of polar, particularly, oxygenated functionality, *i.e.* alcohols and carboxylic acids, on an amorphous/sp^2-embedded surface (Fig. 1).[9] Bottom-up methods, which improve the photoluminescence (PL) properties of the material, involve either surface passivation or heteroatom doping strategies.[8,10] The former provides uniform PL surface trap sites, and is generally achieved *via* amide conjugation of linear diamines (*e.g.* ethylene or polyethylene glycol (PEG)-type diamines) to surface-bound carboxylic acids in either the CD formation step or in a subsequent step.[11] Similarly, the introduction of heteroatoms, especially N, has been shown to improve PL properties especially the quantum yield of fluorescence (QY).[10,12] However, due to the intricate molecular structure of CDs and the lack of knowledge of the

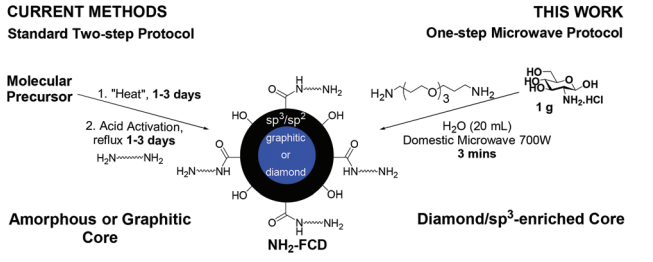

Fig. 1 General syntheses for surface passivated FCDs.

[a]*School of Chemistry, University of Bristol, Cantock's Close, Bristol, BS8 1TS, UK. E-mail: m.c.galan@bristol.ac.uk*
[b]*Cardiff Catalysis Institute, School of Chemistry, Cardiff University, Park Place, Cardiff, CF10 3AT, UK*

†Electronic supplementary information (ESI) available: Detailed protocols, supplementary figures and schemes, toxicity results and confocal microscopy images. See DOI: 10.1039/c6nr07336k

This journal is © The Royal Society of Chemistry 2016

Open Access Article. Published on 21 October 2016. Downloaded on 9/13/2025 2:09:01 PM.
This article is licensed under a Creative Commons Attribution 3.0 Unported Licence.

reaction mechanisms that govern nanoparticle formation and photoluminescence, most methods available are complex and time-consuming; and few large-scale, bottom-up protocols exist that exploit both strategies (surface passivation and N-heteroatom doping) simultaneously. A number of carbohydrates and different nucleation and growth conditions have been reported for the preparation of FCDs, which include glycerol, glycol, glucose, glucosamine, sucrose, dextran, chitosan, cellulose and ascorbic acid as common starting materials.[11,13] However, most methods employ very harsh conditions (chemical or hydrothermal oxidation, pyrolysis, high acidic environments and long reactions times) and require complex post-modifications to improve the surface state of the CDs, followed by lengthy purifications.

As part of our ongoing interest in the development of non-toxic fluorescent nano-platforms for biological applications that are general, practical and accessible to the non-expert at the point of use (*e.g.* biologists and biochemists), we turned our attention to the preparation of water soluble FCDs from low-cost starting materials, that are easily functionalised by a given biomolecule. To that end, glucosamine HCl ($GlcNH_2$·HCl) was chosen as the starting material, as it already contains the required N for nanoparticle doping, and 4,7,10-trioxa-1,13-tridecanediamine (TTDDA)[11,14] as the diamine needed for surface passivation. In addition, the methylene protons in the propyl chain of TTDDA can be used as a ^{1}H-NMR handle to help quantify surface ligands on the FCDs.

The gram-scale synthesis of FCDs was then investigated. An optimal QY of up to 18%, relative to quinine sulfate (Fig. S1A in ESI†),[15] was obtained when $GlcNH_2$·HCl (0.24 M) and TTDDA (1.1 eq.) were reacted in distilled water under microwave (MW) irradiation (domestic 700 W MW) for 3 minutes (Fig. 1, see ESI† for full details). After dissolution in water and sample filtration through a centrifugal concentrator filter with a 10 kDa molecular weight cut-off, amine-coated CDs (NH_2-FCDs) with a strong blue fluorescence under 365 nm UV irradiation (Fig. 2B) and a hydrodynamic volume of 1–10 nm (as measured by dynamic light scattering (DLS)) were obtained (Fig. S2†). High-resolution transmission electron microscopy (HR-TEM) revealed that NH_2-FCDs had an average diameter of 2.45 nm (Fig. 2A). Crystalline structure, with lattice spacings of 0.21 nm and 0.25 nm, was also observed (Fig. S3†). These spacings are consistent with both graphitic [(100), (020)] and diamond-like [(111), (110)] carbon preventing unambiguous structure assignment.[8,19] However, the absence of graphitic (002) spacings of 0.33 nm indicates the NH_2-FCDs may contain predominantly sp^3 enriched carbon. Raman spectroscopy of NH_2-FCDs exhibited two peaks at 660 cm^{-1}, indicative of C–Cl bonds, and 1608 cm^{-1} which deconvoluted to two contributing peaks: a small shoulder centred at 1547 cm^{-1} is symptomatic of sp^2-enriched areas, with the main peak, centred at 1608 cm^{-1}. Being characteristic of strong sp^3 character (Fig. S4A†).[20] Interestingly, the observation of sp^3-enriched crystallinity, instead of the commonly found graphitic or amorphous crystallinity, generated from similar syntheses,[11,13a,21] is to our knowledge the first reported characterisation of a CD with a sp^3-enriched crystalline core fabricated using a bottom-up synthesis.

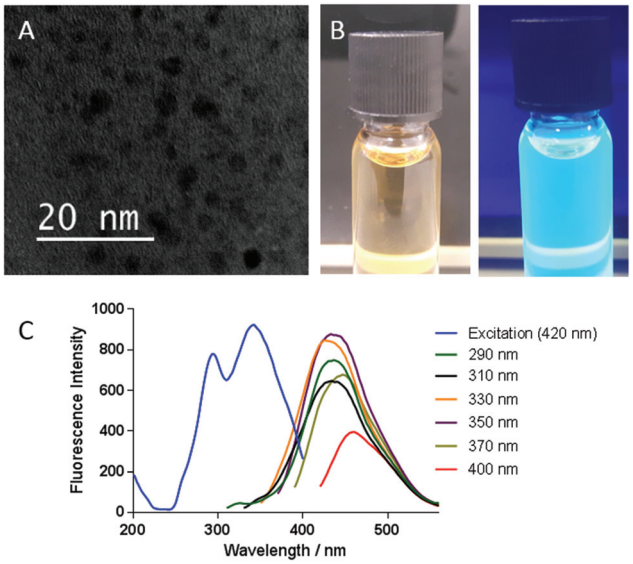

Fig. 2 (A) HR-TEM image of NH_2-FCDs (B) Left: NH_2-FCDs aqueous dispersion in daylight. Right: Irradiated with 365 nm UV light (C) excitation and emission spectrum of NH_2-FCDs.

UV-vis physicochemical characterization of NH_2-FCDs showed an absorbance profile characteristic of CDs from 200–450 nm, with a leading absorbance tail into the near UV region and a defined peak at 270 nm (Fig. S5†). This feature can be attributed to π–π* transition of aromatic/alkenyl C=C bonds or C=N bonds.[16] Moreover, the fluorescence spectroscopy emission profile (excitation 200–400 nm) exhibited the signature features of N-doped CDs, in which there is an excitation-dependent emission (Fig. 2C). The excitation spectrum shows three significant peaks at 200 nm (π–π* of aromatic/alkenyl C=C bonds),[17] 295 and 340 nm (n–π* transitions in C=O/C=N bonds).[18] The excellent photostability of NH_2-FCDs was evaluated and no decrease in emission intensity (at 440 nm) was observed over a 15 hour period of continuous irradiation at 340 nm, whereas an organic fluorophore such as Rhodamine 6G significantly photobleached under similar conditions after 30 min (Fig. S6†). Their chemical inertness was also assessed by monitoring emission over a range of pH values (0–13) (Fig. S7†). Emission intensity was maintained between pH 4–9, and above 70% between pH 1–3 and above pH 10. These results demonstrate the chemical robustness of the newly synthesized NH_2-FCDs.

The composition and chemical functionality present in NH_2-FCDs was then assessed by elemental analysis, Fourier-transformed infra-red (FTIR) and X-ray photoelectron spectroscopy (XPS). Elemental analysis showed a composition of: C, 46.47%; H, 8.33%; N, 7.99%; Cl; 6.51%; and O, 30.70% (Table S1†). FTIR spectrum (Fig. S8†) showed characteristic peaks for the presence of amino or/and alcohol (N–H/O–H) functionalities (signals at 3345 cm^{-1}). Bands at 2974 cm^{-1} indicate the presence of sp^3 C–H, attributable either to

Open Access Article. Published on 21 October 2016. Downloaded on 9/13/2025 2:09:01 PM.
This article is licensed under a Creative Commons Attribution 3.0 Unported Licence.

amorphous carbon or the TTDDA linker. Importantly, surface passivation *via* amide formation is suggested by the presence of an absorption band at 1644 cm^{-1} (NHCO groups). Furthermore, an absorption peak at 1045 cm^{-1} is indicative of C–O ether vibrations, while the band at 625 cm^{-1} corroborates the presence of C–Cl bonds. The wide scan XPS spectrum indicated the presence of C, O, N and Cl (in proportions similar to elemental analysis) with peaks at *ca.* 285 eV (C 1s), 532 eV (O 1s), 400 eV (N 1s) and 197 eV (Cl 2p) (Fig. S9–S11†). Where applicable, high resolution scans of each region were fitted (Table S2†) to reveal further functional group detail. The fitted peaks highlighted the presence of aromatic moieties such as: aromatic C=O and OH groups, aliphatic C=O, imides, and N-heterocycles *e.g.* pyridines.

The electrokinetic potential (zeta potential) of NH_2-FCDs was measured as (−0.08 to +1.64) mV (Fig. S12†). Although a positive charge might be expected due to the presence of distal primary amines from the TTDDA linker, the observed net neutral surface charge can be attributed to other surface functional groups *i.e.* carboxylic acids, esters, alcohols, and bound chlorides. No particle flocculation or coagulation was observed, which suggests that stabilization of NH_2-FCDs might be driven by linker steric effects or the high solubility afforded by the abundance of polar surface functionality.[22]

^{1}H NMR structural characterization of NH_2-FCDs (Fig. S13†) showed two sets of distinct signal intensities associated to FCD surface functionality. Large peaks at 3.6, 2.9 and 1.8 ppm could be assigned to surface bound TTDDA, whilst smaller peaks around 8.5 ppm and 1.5–4.0 ppm correspond to surface-bound aromatic and sp^3-bound protons, respectively. Further analysis by ^{1}H–^{13}C HMBC (Fig. S14†) showed cross-peaks between these lower intensity aromatic and alkyl regions, indicating a patchwork of amorphous and aromatic moieties on the surface of NH_2-FCDs. ^{1}H–^{15}N-HMBC NMR experiments further evidenced desymmetrisation/anchoring of TTDDA onto the surface *via* incorporation into N-containing heterocycles (−160 and −130 ppm) most likely imidazole, pyrazine or pyridine-type molecules (Fig. S15†). Presence of the distal amine was confirmed by the cross-peak at −350 ppm, indicating the presence of ammonium species. Finer NH_2-FCD structural detail can be ascertained by the minor proton species in the ^{15}N NMR spectrum (1.65 and 1.58 ppm) showing cross-peaks at −62 ppm (imine), −253 and −293 ppm (amides) (Fig. S16†).

In order to better understand the molecular mechanisms that lead to NH_2-FCD formation, aliquots of the reaction at 30-second intervals were taken and analysed by FTIR, ^{1}H, ^{13}C, and elemental analysis (Fig. S17–S20†). Loss of the anomeric proton/carbon (^{1}H, ^{13}C NMR) as well as the formation of an aldehyde (FTIR) were observed over the first 90 seconds, after which time the aldehyde disappeared (FTIR) and formation of sp^2-centres/aromatization was then observed (^{1}H, ^{13}C NMR). Additionally, amide formation occurred after 90 seconds (^{13}C NMR, FTIR). Further mechanistic evidence was obtained from qualitative ReactIR studies, under hydrothermal conditions at 70 °C (Fig. S21†).[23] Upon addition of $GlcNH_2$·HCl, to the heated TTDDA solution, two C=O vibrations appeared at 1625 and 1682 cm^{-1} which could be assigned to amide and imine species, respectively. While the imine signal at 1682 cm^{-1} quickly reaches a maximum intensity and then diminishes over time, the amide signal continues to increase before reaching a plateau. Based on these observations, we propose that initial reaction stages involve iminium formation, from reaction of an amine (TTDDA or $GlcNH_2$) with the aldehyde that is generated from ring-opening of the hemiacetal in the carbohydrate moiety. Trapping of the iminium electrophile could allow oligomer formation which, when accompanied by dehydration (as confirmed by elemental analysis of the reaction aliquots at different time points, see Fig. S20†), leads to the formation of the sp^3-enriched nanocrystalline core. In the second phase of the reaction, following the loss of bulk water, further carbonisation occurs and aromaticity is then generated on the outer layers of the sp^3-enriched cores. Surface passivation by TTDDA can now take place *via* either incorporation of TTDDA into the surface heteroaromatics or amide bond formation. Amide formation can occur either through surface bound carboxylic acids reacting directly with an amine (*e.g.* TTDDA or sugar-derived amine) or through the nucleophilic attack of an alcohol to the iminium electrophile, followed by rearrangement of the resulting imidate (Scheme 1).

Functionalisation of NH_2-FCDs with lactose disaccharide, was carried out to highlight the versatility of our FCDs (Scheme 2). Treatment of NH_2-FCDs with succinic anhydride, proceeded by ring-opening, to yield carboxylic acid bearing FCDs (COOH-FCDs), which were then reacted with 1-aminolactose,[6]

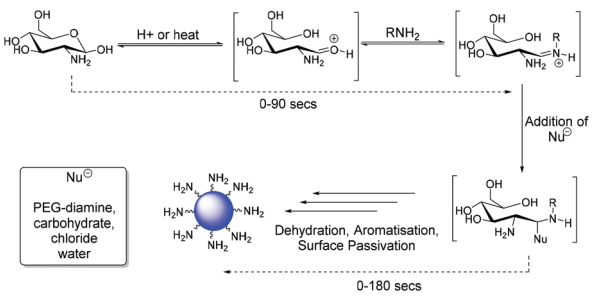

Scheme 1 Proposed mechanism of NH_2-FCD formation.

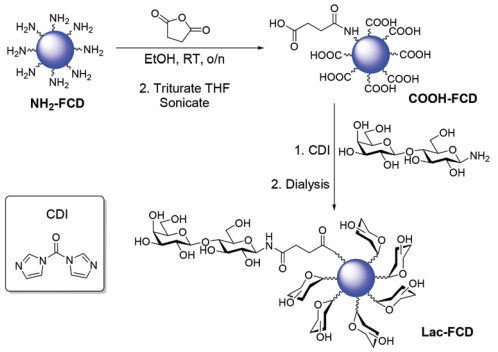

Scheme 2 NH_2-FCDs functionalised to afford COOH/Lac-FCDs.

This journal is © The Royal Society of Chemistry 2016

Open Access Article. Published on 21 October 2016. Downloaded on 9/13/2025 2:09:01 PM.
This article is licensed under a Creative Commons Attribution 3.0 Unported Licence.

in the presence of CDI, to afford lactose-coated CDs (Lac-FCDs). ^{1}H-NMR confirmed the surface functionalization of COOH-FCDs and Lac-FCDs (Fig. S22 and S23†). Interestingly, it was found that the fluorescence properties for COOH/Lac-FCDs were not altered from those of NH_2-FCDs (Fig. S29†).

Cell internalization, and toxicity studies using NH_2-FCDs, COOH-FCDs and Lac-FCD were then performed in HeLa (human cervical) and MDA-MB-231 (human breast) cancer cells. Cultures were exposed to concentrations from 10^{-6} to 2000 μg mL^{-1} for 1 hour, 1, 3 and 7 days.[24] Metabolic competence was assessed by Alamar Blue (AB), and the number of live cells with Calcein AM. The ratio of AB/Calcein affords the reductive metabolism per cell (RMPC), providing a metric to compare treated cells against untreated cells. In MDA (Fig. S30 and S31†), a distinct advantage for lactose-coated FCDs is observed at very high concentrations after 3 and 7 day exposures. NH_2-FCDs and COOH-FCDs show elevated RMPC at concentrations above 500 μg mL^{-1} 3 days and reduced RMPC above 250 μg mL^{-1} 7 days, whereas Lac-FCDs show no significant change from control. In HeLa cells (Fig. S32 and S33†), differences can be seen between differentially functionalised FCDs. NH_2-FCDs show elevated RMPC at 1 hour exposures, with no associated cell death, which is reduced after 1 and 3 days; with significant cell death being seen at concentrations over 250 μg mL^{-1} at 7 days. COOH-FCDs have little toxic effect except at 7 day exposures above 250 μg mL^{-1} where RMPC decreased significantly. Conversely, Lac-FCDs after 3 days, above concentrations of 10^{-1} μg mL^{-1}, show elevated RMPC levels consistently. However, this is not associated with any change in the population size relative to control, and is reduced again after 7 days. These results highlight the utility of the glycan coating to decrease or obviate the toxicity of for FCDs at high concentrations.

Having confirmed the very low toxicity of our novel FCDs, confocal microscopy was used to visualise Lac-FCD's interaction with HeLa (Fig. S34†) and MDA cells (Fig. 3 and S35†). After 2 hour exposure, cells were imaged with 405 nm excitation.[25] It was found that Lac-FCDs were indeed internalised by both cell lines, as determined by *Z*-stack analysis. Compression of a *Z*-stack, that is consecutive sections at different heights within a region of interest, allowed comparison of fluorescence per unit area in treated *vs.* untreated cells. It was found treated cells had a higher total fluorescence than untreated cells (Fig. S34D/35D†). Lac-FCDs generally display a diffuse localisation within the cell in either cell line, with some areas of bright aggregation.

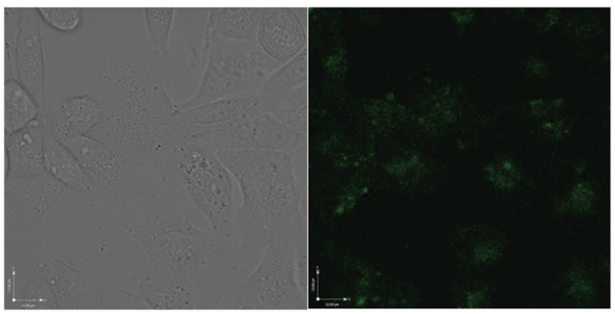

Fig. 3 Confocal microscopy mages of Lac-FCD internalization in MDA cells. Left: Bright Field channel; Right: Fluorescent channel showing Lac-FCDs.

Conclusions

In summary, the facile and expedient MW-assisted synthesis of a novel, sp^3-enriched nanocrystalline and photostable amine-decorated FCD is described (NH_2-FCD) from cheap and available starting materials. The novel NH_2-FCDs consist of a sp^3-enriched crystalline core with an amorphous surface studded with aromatic regions. Mechanistic studies on the formation of NH_2-FCDs suggests the generation of an iminium species which is crucial for carbohydrate degradation and FCD surface passivation. We believe this key step could be exploited to further expand the emission profile of FCDs. Further FCD functionalization to afford non-toxic carboxylic acid and lactose-decorated FCDs (COOH/Lac-FCDs) showed their ease of functionalization. We also demonstrated that Lac-FCDs are readily internalised into human cancer cells with little toxic effect at high concentrations and long exposure times. The simplicity of the protocol and versatility of the FCDs makes this process a valuable addition to the toolbox of chemists and biologists with applications in, and beyond, the field of material chemistry. Moreover, the novel sp^3 nanocrystallinity of these materials, which possess special chemical and physical properties such as high chemical inertness, diamond-like properties, and favorable tribological properties, offers unique opportunities in electrochemical applications and for probing the PL mechanism of FCDs that do not contain sp^2-crystalline regions; these studies are ongoing.

Acknowledgements

This research was supported by EPSRC CAF EP/L001926/1 (MCG), ERC-COG: 648239 (MCG) and EPSRC EP/G036764/1 (SAH). Many thanks to Dr D. Tiwari for Raman help, Dr D. Alibhai (Wolfson Imaging facility) for confocal assistance, and Jon Jones for assistance with TEM studies which were carried out in the Chemistry Imaging Facility with equipment funded by UoB and EPSRC (EP/K035746/1 and EP/M028216/1).

Notes and references

1 K. El-Boubbou and X. F. Huang, *Curr. Med. Chem.*, 2011, **18**, 2060–2078.
2 (*a*) E. Katz and I. Willner, *Angew. Chem., Int. Ed.*, 2004, **43**, 6042–6108; (*b*) M. Marradi, M. Martin-Lomas and S. Penades, *Adv. Carbohydr. Chem. Biochem.*, 2010, **64**, 211; (*c*) C. F. Wu and D. T. Chiu, *Angew. Chem., Int. Ed.*, 2013, **52**, 3086; (*d*) R. Vacha, F. J. Martinez-Veracoechea and

Open Access Article. Published on 21 October 2016. Downloaded on 9/13/2025 2:09:01 PM.
This article is licensed under a Creative Commons Attribution 3.0 Unported Licence.

D. Frenkel, *ACS Nano*, 2012, **6**, 10598; (*e*) I. Canton and G. Battaglia, *Chem. Soc. Rev.*, 2012, **41**, 2718.

3 N. C. Reichardt, M. Martin-Lomas and S. Penades, *Chem. Soc. Rev.*, 2013, **42**, 4358.

4 (*a*) Y. C. Lee and R. T. Lee, *Acc. Chem. Res.*, 1995, **28**, 321; (*b*) C. R. Bertozzi and L. L. Kiessling, *Science*, 2001, **291**, 2357; (*c*) J. J. Lundquist and E. J. Toone, *Chem. Rev.*, 2002, **102**, 555; (*d*) A. Varki and J. B. Lowe, *Essentials of glycobiology*, ed. A. Varki, Cold Spring Harbor, NY, 2009.

5 (*a*) M. S. Hudlikar, X. R. Li, I. A. Gagarinov, N. Kolishetti, M. A. Wolfert and G. J. Boons, *Chem. – Eur. J.*, 2016, **22**, 1415; (*b*) R. Kikkeri, B. Lepenies, A. Adibekian, P. Laurino and P. H. Seeberger, *J. Am. Chem. Soc.*, 2009, **131**, 2110; (*c*) D. C. Kennedy, D. Grunstein, C. H. Lai and P. H. Seeberger, *Chemistry*, 2013, **19**, 3794; (*d*) Y. Yang, M. Yu, T. T. Yan, Z. H. Zhao, Y. L. Sha and Z. J. Li, *Bioorg. Med. Chem.*, 2010, **18**, 5234; (*e*) J. Gallo, N. Genicio and S. Penades, *Adv. Healthcare Mater.*, 2012, **1**, 302; (*f*) P. Di Gianvincenzo, F. Chiodo, M. Marradi and S. Penades, *Methods Enzymol.*, 2012, **509**, 21; (*g*) J. M. De la Fuente and S. Penades, *Biochim. Biophys. Acta, Gen. Subj.*, 2006, **1760**, 636.

6 D. Benito-Alifonso, S. Tremel, B. Hou, H. Lockyear, J. Mantell, D. J. Fermin, P. Verkade, M. Berry and M. C. Galan, *Angew. Chem., Int. Ed.*, 2014, **53**, 810.

7 R. Ray, X. Xu, Y. Gu, H. J. Ploehn, L. Gearheart, K. Raker and W. A. Scrivens, *J. Am. Chem. Soc.*, 2004, **126**, 12736.

8 S. N. Baker and G. A. Baker, *Angew. Chem., Int. Ed.*, 2010, **49**, 6726.

9 S. J. Zhu, Y. B. Song, X. H. Zhao, J. R. Shao, J. H. Zhang and B. Yang, *Nano Res.*, 2015, **8**, 355.

10 Y. Dong, H. Pang, H. B. Yang, C. Guo, J. Shao, Y. Chi, C. M. Li and T. Yu, *Angew. Chem., Int. Ed.*, 2013, **52**, 7800.

11 H. Peng and J. Travas-Sejdic, *Chem. Mater.*, 2009, **21**, 5563.

12 (*a*) Q. Xu, Y. Liu, C. Gao, J. F. Wei, H. J. Zhou, Y. S. Chen, C. B. Dong, T. S. Sreeprasad, N. Li and Z. H. Xia, *J. Mater. Chem. C*, 2015, **3**, 9885; (*b*) Y. L. Wang, Y. Q. Zhao, Y. Zhang, F. Zhang, X. T. Feng, L. Chen, Y. Z. Yang and X. G. Liu, *RSC Adv.*, 2016, **6**, 38761; (*c*) J. Hou, W. Wang, T. Zhou, B. Wang, H. Li and L. Ding, *Nanoscale*, 2016, **8**, 11185.

13 (*a*) H. Zhu, X. Wang, Y. Li, Z. Wang, F. Yang and X. Yang, *Chem. Commun.*, 2009, 5118; (*b*) S. Liu, N. Zhao, Z. Cheng and H. Liu, *Nanoscale*, 2015, **7**, 6836; (*c*) S. K. Bhunia, A. Saha, A. R. Maity, S. C. Ray and N. R. Jana, *Sci. Rep.*, 2013, **3**, 1473; (*d*) J. Hou, J. Yan, Q. Zhao, Y. Li, H. Ding and L. Ding, *Nanoscale*, 2013, **5**, 9558; (*e*) D. Y. Pan, J. C. Zhang, Z. Li, Z. W. Zhang, L. Guo and M. H. Wu, *J. Mater. Chem.*, 2011, **21**, 3565; (*f*) Y. Zhang, X. Liu, Y. Fan, X. Guo, L. Zhuo, Y. Liv and J. Lin, *Nanoscale*, 2016, **8**, 15281; (*g*) Z.-C. Yang, X. Li and J. Wang, *Carbon*, 2011, **49**, 5207.

14 (*a*) H. Peng, Y. Li, C. Jiang, C. Luo, R. Qi, R. Huang, C.-G. Duan and J. Travas-Sejdic, *Carbon*, 2016, **100**, 386; (*b*) Z. A. Qiao, Y. Wang, Y. Gao, H. Li, T. Dai, Y. Liu and Q. Huo, *Chem. Commun.*, 2010, **46**, 8812; (*c*) C. Liu, P. Zhang, F. Tian, W. Li, F. Li and W. Liu, *J. Mater. Chem.*, 2011, **21**, 13163; (*d*) M. Tan, L. Zhang, R. Tang, X. Song, Y. Li, H. Wu, Y. Wang, G. Lv, W. Liu and X. Ma, *Talanta*, 2013, **115**, 950; (*e*) X. Ren, J. Liu, X. Meng, J. Wei, T. Liu and F. Tang, *Chem. – Asian J.*, 2014, **9**, 1054.

15 If free-based $GlcNH_2$ is used under the described conditions, the QY of the NH_2-FCDs drops to below 2% (Fig. S1B†), but the physical structure is unchanged (Raman spectroscopy, Fig. S4B†), suggesting Cl incorporation is paramount for PL properties, possibly acting in a crucial auxochromic manner.

16 H. Ding, J. S. Wei and H. M. Xiong, *Nanoscale*, 2014, **6**, 13817.

17 J. Tan, R. Zou, J. Zhang, W. Li, L. Zhang and D. Yue, *Nanoscale*, 2016, **8**, 4742.

18 Y. H. Yuan, Z. X. Liu, R. S. Li, H. Y. Zou, M. Lin, H. Liu and C. Z. Huang, *Nanoscale*, 2016, **8**, 6770.

19 (*a*) A. Kumar, P. A. Lin, A. Xue, B. Hao, Y. K. Yap and R. M. Sankran, *Nat. Commun.*, 2013, **4**, 2618; (*b*) H. Hirai and K. I. Kondo, *Science*, 1991, **253**, 772.

20 S. Prawer, K. W. Nugent, D. N. Jamieson, J. O. Orwa, L. A. Bursill and J. L. Peng, *Chem. Phys. Lett.*, 2000, **332**, 93.

21 Y. H. Yuan, R. S. Li, Q. Wang, Z. L. Wu, J. Wang, H. Liu and C. Z. Huang, *Nanoscale*, 2015, **7**, 16841.

22 G. Cao, *Nanostructures and Nanomaterials: Synthesis, Properties and Applications*, Imperial College Press, London, 2004.

23 Due to operational considerations, a TTDDA solution was heated to 70 °C, followed by addition of $GlcNH_2$·HCl. Although, quantification is not possible, detection of imine species under these conditions, is highly suggestive of their presence under MW-treatment.

24 It should be noted all FCDs were readily soluble in phosphate-buffered saline (PBS) and all cell media used in cellular experiments. No degradation or aggregation was observed over periods of 7 days at 37 °C or room temperature.

25 Although this excitation is not optimal for Lac-FCDs, the average fluorescence intensity per treated cell was higher in both cell lines (Fig. S32D/S33D†).

This journal is © The Royal Society of Chemistry 2016